ChemComm

Polar-Hydrophobic Ionic Liquid Induces Grain Growth and Stabilization in Halide Perovskites

Journal:	*ChemComm*
Manuscript ID	CC-COM-07-2019-005490.R1
Article Type:	Communication

COMMUNICATION

Polar-Hydrophobic Ionic Liquid Induces Grain Growth and Stabilization in Halide Perovskites

Received 00th January 20xx,
Accepted 00th January 20xx

DOI: 10.1039/x0xx00000x

Dan Liu,[a,b,#] Zhipeng Shao,[c,#] Jianzhou Gui,[a] Min Chen, [b] Mingzhen Liu,[d] Guanglei Cui,[c] Shuping Pang,[c] Yuanyuan Zhou [b]*

The addition of polar-hydrophobic methylammonium trifluoroacetic ionic liquid tailors the hydrophobicity of halide-perovskite precursor solutions and assists the grain growth. This unique additive also functionalizes the grain boundaries via polar-polar interaction, thereby enhancing the optoelectronic properties and chemical stability of perovskites. The resulting perovskite solar cells show high efficiency over 20 % with significantly enhanced ambient stability. This study opens the door to the solution hydrophobicity control towards high-performance perovskite devices.

Hybrid perovskite (HP) materials have recently attracted huge amount of attention in the field of solar cells, primarily because of their outstanding optoelectronic properties and facile solution-processability.[1-3] Since the invention of perovskite-based solar cells (PSCs) by Miyasaka *et al.*, the power conversion efficiency (PCE) of PSCs have climbed rapidly, and now surpassed 24 %.[4] Such swift development of PSCs has been attributed to the advances in understanding the solution chemistry of perovskites, which has led to numerous innovations in processing HP thin films with desirable morphologies and microstructures. In particular, the effects of precursor-solution parameters such as viscosity, compositions, solvent volatility, pH, and solute gelation degree on the perovskite crystallization have been well studied.[5-8] However, in the literature, there are no studies on tailoring the hydrophobicity/hydrophilicity of the precursor solution which is proven in this study to be a very significant parameter that controls the HP solution crystallization. The commonly-used perovskite precursor solutions are made in polar solvents such as dimethylformamide (DMF), dimethyl sulfoxide and *n*-methyl-2-pyrrolidone, and thus exhibit very hydrophilic behavior. This solution hydrophilicity is expected to have a 'double-edged-sword' effect on the HP thin film crystallization. It offers the intrinsic merit of solution-wetting on the substrate, but at the same time leads to high nucleation density and correspondingly high-density grain boundary network in the final thin films.[9,10] Obviously, there are opportunities in achieving large-grain thin films while maintaining the film uniformity through optimizing the hydrophobicity/hydrophilicity of the precursor solution. Note that Qi *et al.*[11] studied the effect of substrate-hydrophobicity on the wetting of the perovskite precursor solution, but this effect may have limited applications to perovskite devices with versatile architectures. In this study, we demonstrate the use of a fluorinated ionic liquid additive, methylammonium trifluoroacetic ($MA^+CF_3COO^-$, MA^+TFA^-) to tailor the intrinsic hydrophobicity of the solution and modulate grain growth of perovskite thin films. MA^+TFA^- clearly differs from other reported additives in its unique polar-hydrophobic nature owing to the $-CF_3$ group. [12] While there may be a family of possible ionic liquids with similar functionality and the ability to tailor the solution hydrophobicity, here MA^+TFA^- serves as the proof-of-concept demonstration of solution-hydrophobicity tailoring here. It is found that MA^+TFA^- addition also chemically functionalizes grain boundaries via polar-polar interaction, leading to the passivation and stabilization of perovskite grains. PSCs processed with the polar-hydrophobic MA^+TFA^- show PCE exceeding 20 % and significantly enhanced ambient stability.

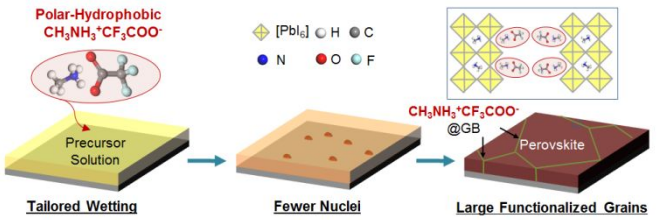

Figure 1. Schematic representation of $MA^+CF_3COO^-$ (MA^+TFA^-) ionic liquid additive mediated crystallization and grain-boundary functionalization of $MAPbI_3$ perovskite thin films.

Figure 1 schematically shows the grain growth and grain-boundary functionalization of $MAPbI_3$ perovskite thin films that are mediated by MA^+TFA^- additive. As seen, MA^+TFA^- contains multiple fluorocarbon groups, which endows this compound with unique polar-hydrophobicity nature. We have confirmed the high solubility of MA^+TFA^- in the DMF as well as the precursor solution (40% in DMF). As shown in Figure S1, 75 wt% of MA^+TFA^- can be fully dissolved in DMF, which is mostly attributed to the high polarity of this compound based on the like-dissolves-like theory.[13] Meanwhile,

[a.] School of Chemistry and Chemical Engineering, Tianjin Polytechnic University, Tianjin 300387, P.R. China
[b.] School of Engineering, Brown University, Providence, Rhode Island 02912, United States; Email: yuanyuan_zhou@brown.edu
[c.] Qingdao Institute of Bioenergy and Bioprocess Technology, Chinese Academy of Sciences, Qingdao 266101, P.R. China;
[d.] School of Materials and Energy, University of Electronic Science and Technology of China, Chengdu 611731, P.R. China.
†Electronic Supplementary Information (ESI) available: Experimental Details, Figures S1 to S12, and Table S1. See DOI: 10.1039/x0xx00000x

the hydrophobicity of MA^+TFA^- tunes the wetting of the precursor solution on the substrate, resulting a high wetting angle and thus reduced heterogeneous nucleation on the substrates. The fewer nuclei grow and coalesce, resulting into $MAPbI_3$ perovskite thin films with low grain-boundary density and large grain size. While the majority of the excess MA^+TFA^- is expected to be released during thermal annealing (see thermo gravimetric analysis of MA^+TFA^- in Figure S2), a small amount of MA^+TFA^- will be trapped at grain boundaries (see evidence later) by interacting with the methylammonium vacancies of grain surfaces, which can be due to the polarity of the MA^+TFA^- molecule. In this context, MA^+TFA^- passivates the traps at grain boundaries, and meanwhile endow the grain boundaries with hydrophobic functionality owing to the fluorocarbon groups. Furthermore, the other components (MA^+ and -COO group) in the MA^+TFA^- additive may be also important which determine the decomposition temperatures as well as molecular-level interactions with perovskite grains.[14]

MA^+TFA^- crystals are synthesized by reacting MA^0 with trifluoroacetic acid, followed by precipitation (see ESI for the detailed synthesis procedure). The structure of the as-synthesized MA^+TFA^- is confirmed with nuclear magnetic resonance (NMR, see Figures S3) and Fourier-Transform infrared spectroscopy (FTIR, see Figures S4). In Figures 2a and 2b, the wetting behaviors of the precursor solution on the substrates (compact-TiO_2-coated FTO-glasses) with and without the MA^+TFA^- addition are compared. The weight ratio of MA^+TFA^- to $MAPbI_3$ is 1:10. As seen, the addition of such a small amount of MA^+TFA^- increases the wetting angles from sub-5^o to 30^o. In Figure S5, it is shown that the wetting angle are continuously increased when more MA^+TFA^- is added, implying an increase in the solution hydrophobicity. The increase in the wetting angle readily causes the growth of large grains in the thin films, as seen in the scanning electron microscope (SEM) images in Figures 2c and 2d. Micrometer-size grains are observed with the addition of MA^+TFA^-. Importantly, the root-mean-square roughness of the thin film, as measured by atomic force microscopy (AFM), shows a similar small value (c.a. 7 nm) to that for the additive-free case (Figures 2e and 2f). We have also studied the effect of MA^+TFA^- adding amount on the final film morphology. We have found that perovskite grains become larger with more MA^+TFA^- addition (Figure S6), and a further increase in $MA^+TFA^-/MAPbI_3$ weight ratio above 1:10 frequently results in incomplete film coverage. These observations are fully consistent with the overall film-growth mechanism in Figure 1. We are also aware that MA^+TFA^- also affect the interfacial energy and chemistry of grain boundaries, which may have an effect on the grain-boundary migration kinetics and contribute to the overall grain growth. X-ray diffraction (XRD) patterns in Figure 2g shows that the high phase-purity of perovskites in both thin films processed with and without MA^+TFA^- additive. In good agreement with the grain growth, the XRD peak intensity is also significantly increased after the MA^+TFA^- addition. X-ray photoelectron spectroscopy (XPS) and energy-dispersive spectroscopy (EDS) measurement were further conducted to exam the fluorine content in the thin films. While most of the MA^+TFA^- additive has been released during the annealing process, a small amount of fluorine (F) is qualitatively from the XPS and EDS results (see Figures S7 and S8). It is deduced that the F element should be located at the grain boundaries of the thin films instead of the crystal structures, as there is no shift in XRD peak positions in Figure 2g. Further evidence for this will be discussed later (Figures 3 and 4). We also envision that high-spatial-resolution elemental analyses of grain boundaries in perovskite thin films based on transmission electron microscopy can be performed in the future, which will be challenging but may provide deterministic understanding of element/phase distributions.[15]

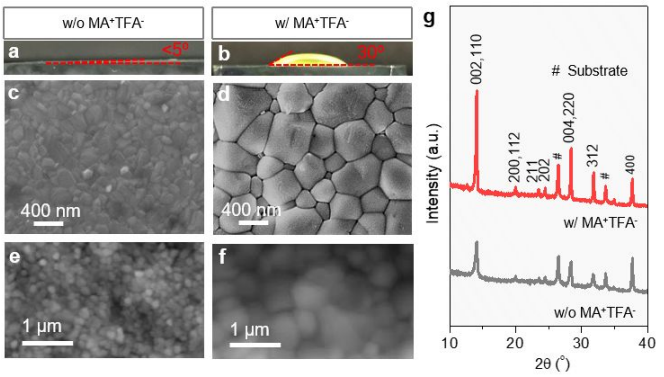

Figure 2. Cross-sectional optical image of $MAPbI_3$ perovskite solution droplets on compact-TiO_2-coated FTO-glasses: (a) without MA^+TFA^- additive; (b) with MA^+TFA^- additive. SEM and AFM images of $MAPbI_3$ perovskite solution droplets on compact-TiO_2-coated FTO-glasses: (c, e) without MA^+TFA^- additive; (d, f) with MA^+TFA^- additive. (g) Indexed XRD patterns of $MAPbI_3$ perovskite thin films made without and with MA^+TFA^- additive. The weight ratio of MA^+TFA^- to $MAPbI_3$ is 1:10.

While the absorption characteristics of the perovskite thin film in Figure S9 basically remain unchanged, the stead-state PL intensity is greatly increased under the same laser excitation condition as shown in Figure 3a. We further performed time-resolved PL spectroscopy to compare the PL lifetime of the thin films with and without MA^+TFA^- additive, and the results are shown in Figure 3b. Both the time-resolved PL spectra can be fit using biexponential functions (see fitting parameters in Table S1), showing average PL lifetimes (τ_{avg}) of 15.6 ns and 6.3 ns for the thin film with and without MA^+TFA^- additive, respectively. The PL results confirm that the trap/defect density in the perovskite thin film is significantly reduced by MA^+TFA^- additive. The trap/defect density reduction is attributed to two factors. First, the solution hydrophobicity leads to the grain growth which reduces the grain-boundary density.[16] Second, the residue MA^+TFA^- that is trapped at the grain boundary passivates the defects/traps.[17-20] Note that the post-annealing condition for preparing the thin film may also influence the grain boundary passivation, which will be systematically studied in the future. We further obtained the time-resolved PL spectrum (Figure S10) of a perovskite thin film (made using solvent annealing) which shows a similar grain size to that of the thin film with MA^+TFA^-. The fit τ_{avg} shows a medium value of 12.2 ns, attesting the positive effect of MA^+TFA^- grain boundary passivation in reducing non-radiative recombination. Furthermore, we compared the electronic properties of the grain boundary in the thin films without and with MA^+TFA^- using conductive AFM, respectively. The schematic illustration for the setup of this measurement is shown in Figure 3c. Current-voltage (*I-V*) curves are obtained at both forward (0V→1.3V) and reverse (1.3V→0V) scans. As seen in Figure 3d, when MA^+TFA^- is present, the overall resistivity of grain boundary is much smaller by simply comparing the slopes of the *I-V* curves. Moreover, *I-V* behavior exhibits negligible hysteresis in the presence of MA^+TFA^- at grain boundaries, which is reproducibly observed for multiple grain boundaries. This is an important sign of trap/defect passivation, because the severe hysteresis at grain boundaries in hybrid perovskite thin films is much related to the abundant defects that can trap carriers or accelerate the ion motions under electric field.[21] We are aware that the grain

boundary misorientation also has some effects on the electronic behavior,[21,22] which can be much less significant than the gain boundary passivation. Based on a rough estimation of the trap-limited voltages from the AFM based *I-V* curves suggests the trap density at the grain boundary is reduced by a factor of two with MA^+TFA^- additive.

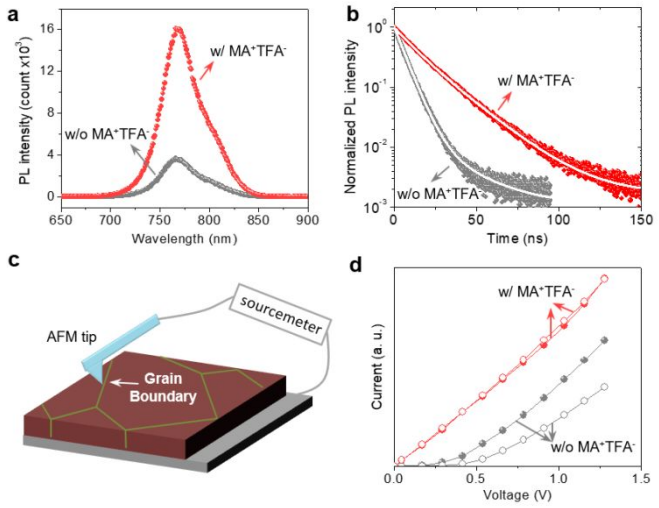

Figure 3. (a) Steady-state and (b) time-resolved PL spectra of $MAPbI_3$ perovskite thin films made without and with MA^+TFA^- additive. (c) Scheme for the *I-V* measurement setup at grain boundaries of the perovskite thin films. (d) *I-V* curves obtained using the setup in (c) for $MAPbI_3$ perovskite thin films made without and with MA^+TFA^- additive. The solid and empty circles represent *I-V* results from forward (bias voltage: 0V → 1.3V) and reverse scans (bias voltage: 1.3V → 0V), respectively. The weight ratio of MA^+TFA^- to $MAPbI_3$ is 1:10.

The MA^+TFA^--functionalized grain boundaries benefit from the intrinsic hydrophobicity of TFA^- ions and endow the thin film with higher tolerance to the ambient moisture. Figures 5a and 5b show the XRD patterns of the $MAPbI_3$ perovskite thin film before and after 48-h exposure to the controlled humid condition of 70% relative humidity (RH) at room temperature (RT). It is seen that the characteristic 001 peak evolves in the MA^+TFA^--free $MAPbI_3$ thin film, indicating that serious decomposition has occurs. In contrast, there is only slight decomposition in the MA^+TFA^- containing $MAPbI_3$ thin film. Then, the surface morphologies of both degraded $MAPbI_3$ perovskite thin films (Figures 4c and 4d) are examined. Note that the perovskite grains in both thin films become coarser due to the long-time moisture exposure.[23] In the MA^+TFA^--free case, the PbI_2 crystals (plate-like) are found to be mainly located at the intergranular regions, which is consistent with the reported phenomena that the grain boundaries are where moisture ingresses and the degradation "nucleates".[14,24,25] After MA^+TFA^- functionalization, it appears that the only slight decomposition of $MAPbI_3$ occurs very randomly and seemingly independent of the grain morphology. These decomposition phenomena are vividly displayed in the insets of Figures 4c and 4d, which is consistent with the fact that the grain boundaries have been functionalized with hydrophobicity and exhibit enhanced moisture resistance, and thus the overall moisture stability.

It is important to note that while the $MAPbI_3$ perovskite composition is studied for the proof-of-concept demonstration, the effect of polar-hydrophobic ionic liquid additive on the grain growth and stabilization is generic to various perovskite compositions. In Figure S11, the results for the thin films with the popularly studied formamidinium lead triiodide ($FAPbI_3$) and mixed-organic-cation $MA_{0.7}FA_{0.3}PbI_3$ perovskite compositions are shown, respectively, again confirming enhanced grain size and stability with MA^+TFA^- functionalization.

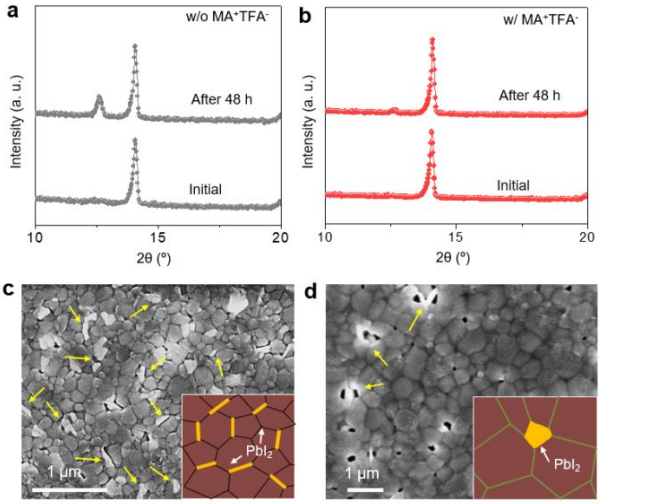

Figure 4. XRD patterns of the $MAPbI_3$ perovskite thin film before and after 48-h exposure to the controlled humid condition (70% RH, RT): (a) without MA^+TFA^- additive; (b) with MA^+TFA^- additive. Top-view SEM images of the degraded $MAPbI_3$ perovskite thin film and the corresponding schematic illustration (inset): (c) without MA^+TFA^- additive; (d) with MA^+TFA^- additive. The weight ratio of MA^+TFA^- to $MAPbI_3$ is 1:10.

PSC devices are then fabricated to evaluate the impact of the MA^+TFA^- additive on the photovoltaic performance of $MAPbI_3$ perovskite thin films. Figure 5a is a cross-sectional SEM image of one typical device made with MA^+TFA^-, showing the device structure clearly. In Figure 5b, the best-performing *J-V* curves (reverse scan) of PSCs made without and with MA^+TFA^- additive are shown. The extracted *J-V* parameters are summarized in the inset of Figure 6b. The overall PCE increases from 17.9 % to 20.1% after the MA^+TFA^- addition, and the most obviously improved parameter is open circuit voltage (V_{OC}) that increases from 1.07 V to 1.15 V. This is consistent with the suppression in non-radiative recombination in the perovskite thin films made with MA^+TFA^- as suggested by the PL results. The typical *J-V* hysteresis for both devices are compared in Figure S12. It is obviously seen that MA^+TFA^- reduces the hysteresis, which is consistent with the result in Figure 3d and attests the grain boundary passivation effect. For the PSC with MA^+TFA^-, the stabilized PCE output monitored at the maximum power point (determined from the reverse *J-V* scan) is shown in Figure 5c, delivering a stable value of about 19.4%. The PCE statistics in Figure 5d confirms the high reproducibility of the PCE enhancement by the MA^+TFA^- addition. Figure 5e compares the ambient-stability of the typical PSCs made without and with MA^+TFA^- additive. After 336 h of storage in the controlled ambient environment (40 % RH, RT), the MA^+TFA^--functionalized PSC show an impressively small decay of only 11%, compared to 38% for MA^+TFA^-free case. While all the device results have proven the efficacy of the MA^+TFA^- approach, PSCs with the state-of-the-art perovskite compositions will be fabricated in the future for higher PCE, and more standardized tests will be performed to fully evaluate the effect of MA^+TFA^- functionalization on the operational stability of PSC devices.[26]

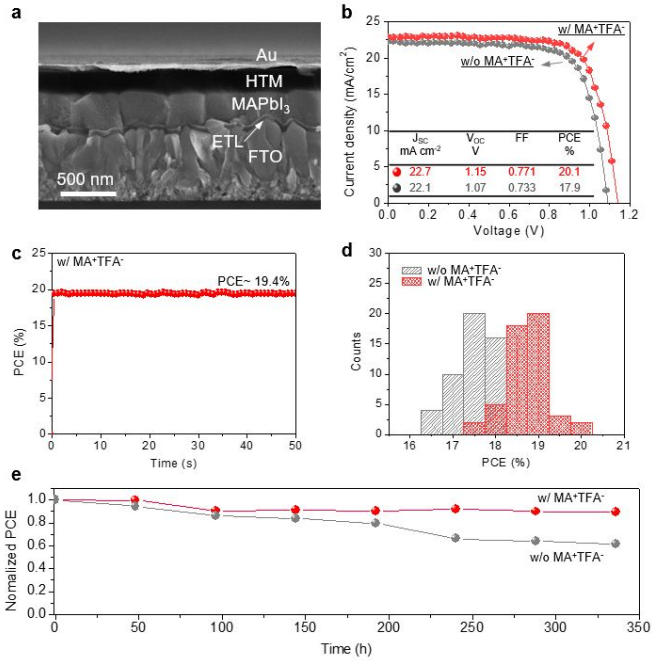

Figure 5. (a) Cross-sectional SEM image of one typical PSC device made with MA^+TFA^-. (b) *J-V* curves of the best PSCs made without and with MA^+TFA^- additive. Inset shows the extracted *J-V* parameters. (c) The stabilized PCE output at maximum power point of the PSC made with MA^+TFA^- additive. (d) PCE statistics of the typical PSCs made without and with MA^+TFA^- additive. (e) Ambient-stability plots of the typical PSCs made without and with MA^+TFA^- additive. The weight ratio of MA^+TFA^- to $MAPbI_3$ is 1:10.

Conclusions

We have demonstrated the use of polar-hydrophobic ionic liquid additive to tune the wetting of precursor solution on the substrate and tailor the crystallization behavior for hybrid perovskite thin films. The additive not only modulates growth of the grains and reduces grain boundaries, but also functionalize grain boundaries in the final thin films, making the perovskite phase much more stable. This polar-hydrophobic ionic liquid induced grain growth and stabilization contributes to higher efficiency and better stability in perovskite solar cell devices. The reported chemical behavior is not limited to the application to solar cells, but a wide range of (opto)electronic devices that demands low defect density. This work here represents a new direction in enhancing the thin film properties and device performance of halide perovskites.

Acknowledgements

The funding from the National Science Foundation (No. OIA-1538893) and Office for Naval Research ((N00014-17-1-2232) are acknowledged. We also thank the support from Advanced Ceramics and Nanomaterials Laboratory led by Prof. Nitin P. Padture.

Conflicts of interest

There are no conflicts to declare.

Notes and references

[1] Y. Rong, Y. Hu, A. Mei, H. Tan, M. I. Saidaminov, S.I. Seok, M. D. McGehee, E. H. Sargent, H. Han, *Science*, **2018**, *361*, eaat8235.
[2] M. Lee, J. Teuscher, T. Miyasaka, T. N. Murakami, H. J. Snaith, *Science* **2012**, *338*, 643.
[3] A. Kojima, K. Teshima, Y. Shirai, T. Miyasaka, *J. Am. Chem. Soc*. **2009**, *131*, 6050-6051.
[4] https://www.nrel.gov/pv/cell-efficiency.html (accessed in Aug. 11, 2019)
[5] J. Hamill, Jr, J Schwartz, L. Loo, *ACS Energy Lett*. **2018**, *3*, 92.
[6] Y. Zhou, M. Yang, W. Wu, A. L. Vasiliev, K. Zhu, N.P. Padture, *J. Mater. Chem*. A **2015**, *3*, 8178-8184.
[7] N.K. Noel, M. Cogiu, A. J. Ramadan, S. Fearn, D. P. McMeekin, J. B. Patel, M. B. Johnston, B. Wenger, H. J. Snaith, *Joule* **2017**, *1*, 328-343.
[8] D. H. Shen, X. Yu, X. Cai, M. Peng, Y. Z. Ma, X. Su, L. X. Xiao, D. C. Zou, *J. Mater. Chem. A*, **2014**, *2*, 20454-20461.
[9] Y. Zhou, O. S. Game, S. Pang, N. P. Padture, *J. Phys. Chem. Lett.* **2015**, *6*, 4827-4839.
[10] W.A. Dunlap-Shohl, Y. Zhou, N.P. Padture, D.B. Mitzi, *Chem. Rev*., 2019, 119, 3193-3295.
[11] C. Bi, Q. Wang, Y. Shao, Y. Yuan, Z. Xiao, J. Huang, *Nat. Commun*. **2015**, *6*, 7747
[12] (a) J.C. Biffinger, H.-W. Kim, S. G. DiMagno, *ChemBioChem* **2004**, *5*, 622-627; (b) D. Yang, X. Zhou, R. Yang, Z. Yang, W. Yu, X. Wang, C. Li, S. Liu, R.P.H. Chang, *Energy Environ. Sci.* **2016**, *9*, 3071-3078; (c) D. Yang, R. Yang, X. Ren, X. Zhu, Z. Yang, C. Li, S. Liu, *Adv. Mater*., **2016**, *28*, 5206-5213.
[13] L. Pauling, *General Chemistry (Dover Books on Chemistry)*, Dover Publications, 3rd Revised ed. Edition, **1988**.
[14] L. Chao, Y. Xia, B. Li, G. Xing, Y. Chen, W. Huang, *Chem* **2019**, 5, 995-1006.
[15] Y. Zhou, H. Sternlicht, N.P. Padture, *Joule* **2019**, 3, 641-661.
[16] F. Ji, S. Pang, L. Zhang, Y. Zong, G. Cui, N.P. Padture, Y. Zhou, *ACS Energy Lett*. **2017**, *2*, 2727-2733.
[17] X. Zheng, B. Chen, J. Dai, Y. Fang, Y. Bai, Y. Lin, H. Wei, Z. Cheng, J. Huang, *Nat. Energy* **2017**, *1*, 17102.
[18] T. Niu, J. Lu, R. Munir, J. Li, D. Barrit, X. Zhang, H. Hu, Z. Yang, A. Amassian, K. Zhao, A. Liu, *Adv. Mater.* **2018**, *30*, 1706576.
[19] Y. Zong, Y. Zhou, Y. Zhang, L. Zhang, M.-G Ju, M. Chen, S. Pang, X. C. Zeng, N.P. Padture, *Chem* **2018**, *4*, 1404-1415.
[20] Q. Chen, H. Zhou, Y. Fang, A.Z. Stieg, T.-B. Song, H.-H. Wang, X. Xu, Y. Liu, S. Lu, J. You, P. Sun, J. Mckay, M.S. Goorsky, Y. Yang, *Nat. Commun*. **2015**, 6, 7269
[21] Y. Shao, Y. Fang, T. Li, Q. Wang, Q. Dong, Y. Deng, Y. Yuan, H. Wei, M. Wang, A. Gruverman, J. Shield, J. Huang, *Energy Environ. Sci.* **2016**, *9*, 1752-1759.
[22] S. Jariwala, H. Sun, G.W.P. Adhyaksa, A. Lof, E.C. Garnett, D.S. Giner, **2019** arXiv:1903.11033.
[23] J. Huang, S. Tan, P.D. Lund, H. Zhou, *Energy Environ. Sci.* **2017**, 10, 2284-2311
[24] Q. Wang, B. Chen, Y. Liu, Y. Deng, Y. Bai, Q. Dong, J. Huang, *Energy Environ. Sci.* **2017**,*10*, 516-522.
[25] A. Gomez, S. Sanchez, M. Campoy-Quiles, A. Abate, *Nano Energy* **2018**, 45, 94-100.
[26] M. Saliba, *Science* **2018**, 359, 388-389

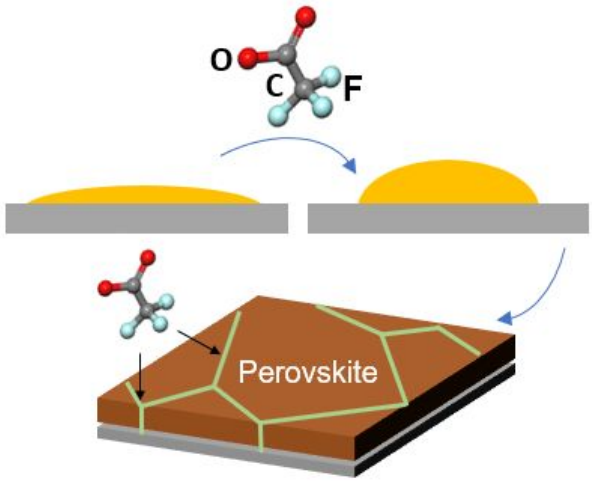

Large Functionalized Grains

Polar-hydrophobic ion liquid additive enlarges and functionalizes perovskite grains.